Full Paper

Electroanalytical Responses of Arsenic Oxide, Methanol, and Oxygen at the Ruthenium Oxide – Hexachloroiridate with Platinum Hybrid Film

Umasankar Yogeswaran, Shen-Ming Chen, Sheh-Hung Li*

Department of Chemical Engineering and Biotechnology, National Taipei University of Technology, No. 1, Section 3, Chung-Hsiao East Road , Taipei 106, Taiwan (ROC)
*e-mail: smchen78@ms15.hinet.net

Received: April 21, 2008
Accepted: July 31, 2008

Abstract
Electrochemically active ruthenium oxide ($RuO_x \cdot nH_2O$), ruthenium oxide/hexachloroiridate ($RuO_x \cdot nH_2O/IrCl_6^{2-}$), and ruthenium oxide/hexachloroiridate/platinum ($RuO_x \cdot nH_2O/IrCl_6^{2-}$/Pt) hybrid films have been prepared from the mixture of Ru^{3+}, $IrCl_6^{2-}$, and $PtCl_6^{2-}$ ions in an acidic aqueous solution. The repetitive cyclic voltammetry (CV) has been used for the film preparation process. The electrochemical properties and the growth mechanism of the above mentioned different kinds of hybrid films have been investigated using CV and electrochemical quartz crystal microbalance. The morphological and quantitative analyses have been carried out using scanning electron microscopy, atomic force microscopy and energy dispersive X-ray. Among these above mentioned films, $RuO_x \cdot nH_2O/IrCl_6^{2-}$/Pt hybrid film exhibits promising electrocatalytic activity towards the oxidation of arsenic oxide, methanol and reduction of oxygen. Further, detailed study of electrocatalysis using rotating ring disk electrodes and amperometric methods have been carried out for arsenic oxide oxidation and oxygen reduction reactions at the hybrid films. From the results, the sensitivity of $RuO_x \cdot nH_2O/IrCl_6^{2-}$/Pt hybrid film has been calculated for arsenic oxide as 0.7 mA mM^{-1}; and for oxygen as 1.8 mA mM^{-1}.

Keywords: Ruthenium oxide, Hexachloroiridate, Platinum, Modified electrodes, Electrocatalysis

DOI: 10.1002/elan.200804322

1. Introduction

Platinum (Pt), ruthenium (Ru), and iridium hybrid materials received great attention in the last few years as high specific surface anodes for electrochemical sensor applications [1 – 10]. It is a known fact that, the direct electrochemical behavior of bare glassy carbon (GC) electrode does not show relatively large difference of peak potentials; also the formed sensors show very low sensitivity. To overcome this limitation, several steps had been taken for the fabrication of metal oxides and metal particle hybrid materials, which have been used for enhancing sensing applications. Such kind of materials includes gold [11, 12], SiO_2 nanoparticles, etc [13, 14]. Among these materials, metal oxide electrodes have shown some advantages in electrochemical analysis; and micro or nano metal oxides exhibit unique performance in electric, optical, magnetic and catalytic aspects [15]. Ruthenium based ferrocyanides had also been used as potential electrode material for the electroanalysis, electrocatalysis [16 – 18], electrochromism [19], ion-exchange reactions [20], photoelectrochemical, photocatalytic devices, batteries and capacitors [21].

Suffredini et al. [22] recently adapted a sol-gel coating technique for easy preparation of electrochemically active Pt-RuO_2-carbon electrodes, which was mainly used for flat surface substrates [23 – 25]. The experimental results obtained with these composites supported on GC shown a higher activity towards methanol electrooxidation than the commercial state of art catalysts with similar Pt-Ru loading. It should be stressed, that the GC substrates exhibit good stability, as opposed to other electrode materials like titanium and gold that form oxides at the higher anodic potentials. Despite of the special advantages related to the use of the sol-gel method to produce oxide coatings [26], little attention has been given to its use for the production of catalytic films. Some applications of above mentioned method have been published, particularly those aiming to produce oxide powders [27 – 29] or films onto titanium substrates [30, 31]. On the other hand, RuO_2-IrO_2 mixed oxide electrodes were amongst the most studied materials for oxygen evolution in acid media. In those systems, the presence of iridium improves the stability of RuO_2, and acts as a very efficient catalyst [32 – 34].

Arsenic is one of the most toxic elements for living beings found in nature. It constitutes one of the main concerns in relation to human health. Consumption of water with high concentrations of arsenic over an extended period of time causes serious diseases especially in rural and semi-urban areas, where water irrigates food or drinking water is often used without treatment. The diseases includes the develop-

ment of cardiovascular and peripheral vascular disease anomalies, neurological and neurobehavioral disorders, diabetes, hearing loss, portal fibrosis of the liver, lung fibrosis, hematological disorders, and carcinoma [35–39]. As a consequence, the necessity of the arsenic detection and the development of sensors becomes wide interest. In the previous literature, for arsenic detection, various metal oxides and specific dye modified electrodes have been used [40–42]. Other than arsenic, the development of the catalysts towards the reduction of oxygen has been much focused in the development of fuel cells and batteries [43]. Various metal macrocyclic complexes have been used for the electrocatalysts for the reduction of oxygen in the acidic and alkaline solutions [44, 45]. Similarly, methanol has also been widely used in the direct methanol fuel cells at lower temperatures, where the methanol oxidation was done with the help of metal oxide catalysts [46, 47]. In our present work, a new type of ruthenium oxide/hexachloroiridate/platinum hybrid film has been prepared using repetitive cyclic voltammetry (CV) and used for the electrocatalysis of arsenic, methanol and oxygen. The scanning electron microscopy (SEM) and atomic force microscopy (AFM) techniques have been used for morphological characterizations of the prepared hybrid films.

2. Experimental

2.1. Materials and Apparatus

Ruthenium (III) chloride, potassium hexachloroiridate and potassium hexachloroplatinate were obtained from Aldrich and were used as received. All other chemicals used were of analytical grade. The preparation of aqueous solutions was done with twice distilled deionized water. Solutions were deoxygenated by purging with pre-purified nitrogen gas. Buffer solutions were prepared from 0.1 M KNO_3 for pH 2.0 aqueous solutions. Cyclic voltammetry (CV) and rotating ring disk electrode (RRDE) were performed in an analytical system model CHI-400 and CHI-750 potentiostat connected to a model AFMSRX analytical rotator respectively. The RRDE electrode was purchased from Pine Instrument Co., which consists of glassy carbon disk electrode and platinum ring electrode. A conventional three-electrode cell assembly consists of Ag/AgCl reference electrode and Pt wire counter electrode were used for the electrochemical measurements. The working electrode was either an unmodified GC or a GC modified with the hybrid films; all the potentials have been reported versus Ag/AgCl reference electrode. The working electrode for EQCM measurements was an 8 MHz AT-cut quartz crystal coated with gold. The diameter of the quartz crystal is 13.7 mm; the gold electrode diameter is 5 mm. The morphological characterization of hybrid films was examined by means of SEM (Hitachi S-3000H) and AFM (Being Nano-Instruments CSPM4000). The quantitative analysis of the films has been examined using energy dispersive x-ray (EDX) analysis (Horiba 7021-H). All the measurements were carried out at 25 °C (±2).

2.2. Preparation of $RuO_x \cdot nH_2O$, $RuO_x \cdot nH_2O/IrCl_6^{2-}$ and $RuO_x \cdot nH_2O/IrCl_6^{2-}$/Pt Hybrid Films

Before starting each experiment, GCs were polished by BAS polishing kit with 0.05 μm alumina slurry, then rinsed and then ultrasonicated in double distilled deionized water. The electrochemical formation of ruthenium oxide ($RuO_x \cdot nH_2O$), ruthenium oxide/hexachloroiridate ($RuO_x \cdot nH_2O/IrCl_6^{2-}$) and ruthenium oxide/hexachloroiridate/platinum ($RuO_x \cdot nH_2O/IrCl_6^{2-}$/Pt) hybrid films were performed by continuous cycling of potential at the working electrode. The continuous cycling has been performed in a defined potential range, using a suitable scan rate in 0.1 M KNO_3 aqueous solution at pH 2.0, which contains Ru^{3+}, $IrCl_6^{2-}$ and $PtCl_6^{2-}$ ions. In detail, two different methods were followed for the preparation of $RuO_x \cdot nH_2O/IrCl_6^{2-}$/Pt hybrid film. The first preparation method of $RuO_x \cdot nH_2O/IrCl_6^{2-}$/Pt hybrid film (hybrid-I) involves the deposition of Pt on GC to form an electroactive film from a pH 2.0 acidic aqueous solution containing $PtCl_6^{2-}$ ions. This deposition was followed by the deposition of $RuO_x \cdot nH_2O/IrCl_6^{2-}$ on the Pt modified GC at similar conditions, using the solution containing Ru^{3+}, $IrCl_6^{2-}$ ions (potential range = 1.1 to −0.1 V). The second preparation method of $RuO_x \cdot nH_2O/IrCl_6^{2-}$/Pt hybrid film (hybrid-II) involves the simultaneous deposition of $RuO_x \cdot nH_2O$, $IrCl_6^{2-}$ and Pt on GC at similar conditions using the solution containing Ru^{3+}, $IrCl_6^{2-}$ and $PtCl_6^{2-}$ ions (potential range = 1.1 to −0.3 V).

3. Results and Discussion

3.1. Electrochemical Preparation and Characterization of $RuO_x \cdot nH_2O$, $RuO_x \cdot nH_2O/IrCl_6^{2-}$, Hybrid-I and II Films

Hydrous RuO_x film has been deposited on GC from 0.01 M $RuCl_3.xH_2O$ present in 0.1 M KNO_3 pH 2.0 electrolytic solution. The typical cyclic voltammograms for the growth of $RuO_x \cdot nH_2O$ film shows two set of redox peaks in the potential range of −0.2 to 0.9 V (figure not shown). During the negative scan, a peak appeared at 0.35 V, which is due to the reduction of Ru^{3+} and thus the deposition of ruthenium (Ru) has taken place on the GC electrode. On the positive sweep, the deposited Ru oxidized to hydrous oxides ($RuO_x \cdot nH_2O$) and hydroxyl Ru^{4+} species and their corresponding peaks have appeared at about 0.8 V; and the redox couple at $E^{\circ\prime} = 0.2$ V represents the $Ru^{1+/2+}$ redox reaction [48]. Following the above growth studies of $RuO_x \cdot nH_2O$, the $RuO_x \cdot nH_2O/IrCl_6^{2-}$ film have also been deposited on GC at similar pH (0.1 M KNO_3 pH 2.0) using the solution containing Ru^{3+} and $IrCl_6^{2-}$ ions. The concentration of Ru^{3+} and $IrCl_6^{2-}$ used in the mixture was 5 and 0.6 mM respectively, and the scanning potential region for film growth is 1.0 to −0.1 V (figure not shown). In this above experiment, upon continuous cycling, the redox peak currents appeared at the formal potentials $E^{\circ\prime} = 0.7$, 0.25 and 0.35 V has found to be increasing. This behavior

indicates the deposition of $RuO_x \cdot nH_2O/IrCl_6^{2-}$ film during cycling. The redox couple at $E^{\circ\prime} = 0.7$ V could be proposed as the redox reactions of both $RuO_x \cdot nH_2O$ and $IrCl_6^{2-}$ present in the film, and the $E^{\circ\prime} = 0.25$ and 0.35 V redox couple represents only $RuO_x \cdot nH_2O$ present in the film. The deposition of Pt on GC has also been studied under similar conditions using the solution containing $PtCl_6^{2-}$ ions (0.8 mM). The scanning potential region of the Pt deposition is between 1.1 and −0.3 V (figure not shown). Upon continuous cycling, the peak currents of the two redox couples appeared at $E^{\circ\prime} = 0.6$ V and −0.2 V have found to be increasing, which represents the deposition of platinum during cycling. The electrochemical reaction at 0.4 V can be explained as the reduction of $Pt^{II}Cl_6^{4-}$ to Pt on the GC surface. As explained in the experimental section, two types of hybrid films have been studied, hybrid-I (figure not shown) and hybrid-II films. Figure 1A represents the growth of the hybrid-II film. Comparison of hybrid-I and II films reveals that the redox currents for hybrid-II are higher than that of hybrid-I film. This above result represents that the hybrid-II film is more electrochemically active than hybrid-I film. The composition ratio of materials in the different films may also be varied, which have been confirmed by detailed electrochemical studies, EDX spectrum and microscopic studies in the following sections.

The electrochemical behavior of $RuO_x \cdot nH_2O$, $RuO_x \cdot nH_2O/IrCl_6^{2-}$, hybrid-I and II film modified GC electrodes have been studied after washing them in double distilled deionized water, and transferring them in to pH 2.0 aqueous H_2SO_4 solution. Figure 1B represents the electrochemical behavior of $RuO_x \cdot nH_2O$ film modified GC electrode, where the overlapped redox couples at $E^{\circ\prime} = 0.38$ and 0.2 V obviously reveals the redox reactions of $Ru^{3+/4+}$ and $Ru^{1+/2+}$ at $RuO_x \cdot nH_2O$ film respectively. Similarly, Figure 1C shows the redox couples of $RuO_x \cdot nH_2O/IrCl_6^{2-}$ film modified GC, where the $E^{\circ\prime}$ at 0.31 and 0.46 V represents the redox reactions of $RuO_x \cdot nH_2O/IrCl_6^{2-}$ film. In the same figure, the peak at 0.84 V represents the reduction peak current of $IrCl_6^{2-}$ present in the $RuO_x \cdot nH_2O/IrCl_6^{2-}$ film. Similarly, the Pt modified GC electrode has also been studied in pH 2.0 aqueous H_2SO_4 solution as shown in Figure 1D. In this result, the redox peaks at $E^{\circ\prime} = -0.08$ and −0.18 V represents the hydrogen adsorption and desorption. The oxidation and reduction peak at 0.82 and 0.46 V represents the redox reaction of Pt. Further, a comparative study of hybrid-I and II film have been conducted at similar conditions to that of above mentioned films. The results reveal that the hybrid-II film possess higher current than hybrid-I film for $RuO_x \cdot nH_2O$ and $IrCl_6^{2-}$ as shown in Figure 1E, where the reduction peak currents $E_{pc} = 0.2$, 0.42 and 0.83 V at (a) are higher than (b). This is due to the higher deposition of $RuO_x \cdot nH_2O$ and $IrCl_6^{2-}$ in the hybrid-II film. These results have been given in Table. 1 in the form of surface coverage concentration values (Γ). In this calculation, the charge involved in the reaction (Q) has been obtained from CVs and applied in the equation $\Gamma = Q/nFA$ where, n is the number of electron transfer involved for a redox reaction. A detailed study of the same has been carried out in the following section using EDX analysis to determine the various elements present in the various films. Following these above studies, the effect of scan rate for all the films have also been carried out at similar conditions as that of above mentioned experiments (figures not shown). From these results, the value of $\Delta E_p = (E_{pc} - E_{pa})$ obtained is small, but it is non-zero when the scan rate is between 10 and 200 mV s^{-1}. This can be explained as the proton transfer capability of the redox reactions of all the four films. The plots of I_{pa} versus the scan rate (not shown in figures) illustrates a close linear dependence of I_{pa} and I_{pc} on the scan rates value. This behavior is found to be consistent with a thin layer reversible electron transfer process for scan rates between 10 and 200 mV s^{-1} for all the four films. Further, this above result is also found to be consistent with diffusion less and reversible electron transfer process at lower scan rates. The peak current and scan rate are related as follows

$$I_p = n^2F^2vA\Gamma_o/4RT \quad (1)$$

Where, Γ_o, v, A, and I_p represents the surface coverage concentration, scan rate, electrode area and the peak current, respectively. However, both I_{pa} and I_{pc} have close linear dependence on the scan rate, indicative of a reversible electron transfer process of the film. Based on these above results (Fig. 1) and because of the lower in peak currents for hybrid-I film, hybrid-I film has been excluded in the following electrochemical studies.

The pH effect on hybrid-II has been studied; it shows the electrochemical behavior of hybrid-II film in various pH aqueous buffer solutions. The preparation of the film for these studies has been done as mentioned in the experimental section. These results shows interesting electrochemical properties by having two components with peak potentials, which has either a pH effect ($RuO_x \cdot nH_2O$ and Pt) or pH independent ($IrCl_6^{2-}$). The CVs of the hybrid-II film has been carried out at pH 0.5, 2.0, 2.5, 2.8 and 5 (figures not shown). The results show that the formal potential of Pt depends on pH, and that the formal potential of $IrCl_6^{2-}$ at 0.7 V is effectively independent of the pH, which reveals that Pt exhibits proton transfer in the redox reaction. Similarly, the redox couples of $RuO_x \cdot nH_2O$ of hybrid-II film at 0.25 and 0.35 V also exhibit change in peak potentials in different pH solutions. For both $RuO_x \cdot nH_2O$ and Pt, the response (peak potential vs. pH) shows the slope of −79 mV/pH, which is close to that given by the Nernstian equation for equal number of electrons and protons transfer.

3.2. EQCM Studies of $RuO_x \cdot nH_2O/IrCl_6^{2-}$, Pt, and Hybrid-II Films

The change in CVs along with the EQCM frequency resulting from the growth of $RuO_x \cdot nH_2O/IrCl_6^{2-}$ film, only Pt film and hybrid-II film on the gold electrodes have been studied (figures not shown). The film formations and the experimental conditions for the gold electrodes are

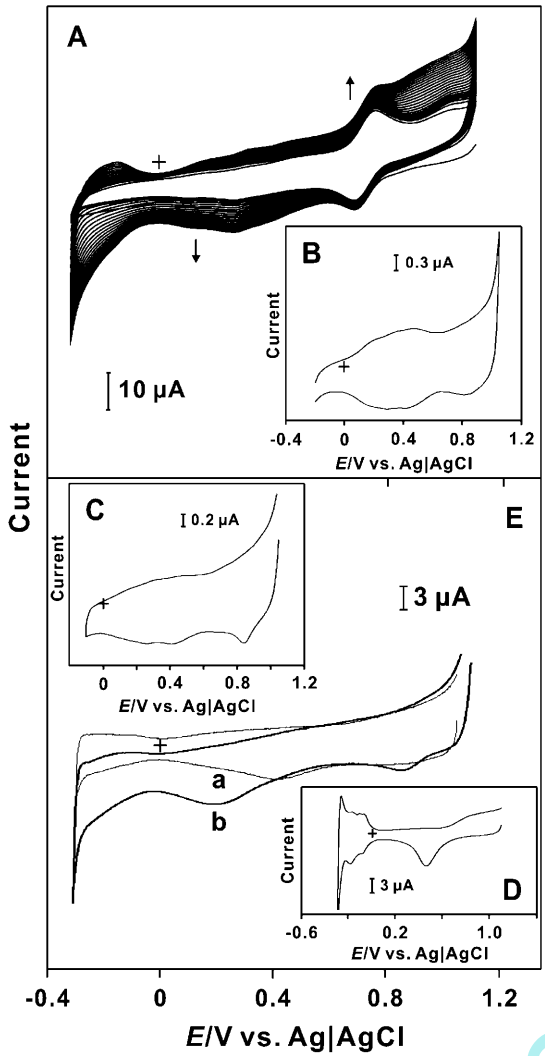

Fig. 1. A) Repetitive CVs of Hybrid-II modified GC from 1×10^{-2} M $RuCl_3$, 1.5×10^{-3} M K_2IrCl_6 and 8×10^{-4} M K_2PtCl_6, at the potential range of 1.1 and -0.3 V, scan rate is 100 mV s^{-1}. CVs of B) $RuO_x\cdot nH_2O$, C) $RuO_x\cdot nH_2O/IrCl_6^{2-}$, D) Pt, E)a) hybrid-I and b) hybrid-II film modified GCs, scan rate is 20 mV s^{-1}. The peak currents reveal that hybrid-II is more electroactive than all other films. For all the above experiments, the potentials measured vs. Ag/AgCl, and the 0.1 M KNO_3 pH 2.0 aqueous solution as electrolyte has been used.

Table 1. Surface coverage concentrations (Γ) of various species at different film modified GCEs in pH 2.0 aqueous H_2SO_4 solution.

Film type	Γ (pmol cm^{-2})			
	Ru^{1+}	Ru^{3+}	$IrCl_6^{2-}$	Pt
$RuO_x\cdot nH_2O$	523	275	–	–
$RuO_x\cdot nH_2O/IrCl_6^{2-}$	53.4	131	35.9	–
Only Pt	–	–	–	4130
Hybrid-I	No peak	8.78	11.3	1440
Hybrid-II	770	1950	193	1140

similar to that of GC. From the CVs and EQCM frequency change due to $RuO_x\cdot nH_2O/IrCl_6^{2-}$ film deposition, the potential range of the $RuO_x\cdot nH_2O$ deposition is found to be 0 to 0.6 V, which exhibits three redox couples at 0.4, 0.3 and 0.16 V. The peak currents for $IrCl_6^{2-}$ film formation appeared at 0.9 V. The overall corresponding frequency change for $RuO_x\cdot nH_2O/IrCl_6^{2-}$ film formation can be observed at the potential range of 0.6 to 0.9 V. From these EQCM results, the frequency change observed at 0.6 V to 0.9 V is higher than that of 0 to 0.6 V potential range. This phenomenon indicates that the amount of $IrCl_6^{2-}$ film formed must be higher when comparing with $RuO_x\cdot nH_2O$ deposition in the $RuO_x\cdot nH_2O/IrCl_6^{2-}$ film formation. This result is consistent with the comparison of Fig. 1(B) with (C), where the peak current of $RuO_x\cdot nH_2O$ is higher in Fig. 1(B) than in (C). The CVs and EQCM frequency change due to Pt film deposition, shows that the deposition of Pt film occurred in the potential range of 0.2 to -0.3 V. In the Pt deposition process, $Pt^{II}Cl_6^{4-}$ has been reduced to Pt on the gold electrode surface. In this, the Pt deposition started at 0.2 V and most deposition occurred at negative potential than that of 0.2 V. However, at the second cycle, the deposition potential shifted 100 mV more positive than that of the earlier one. This result indicates that, the deposition of Pt occurred on Pt covered gold surface from the second cycle. Similar to the above discussed films ($RuO_x\cdot nH_2O/IrCl_6^{2-}$ and Pt), the frequency change due to the hybrid-II film can be observed at potential ranges of 0.8, -1.0 V and 0, -0.3 V, which indicates that the amount of $RuO_x\cdot nH_2O$ and $IrCl_6^{2-}$ deposited was higher in hybrid-II film when comparing other two films. The change in mass at the quartz crystal has been calculated from the change in the observed frequency using the Sauerbrey equation

$$\text{Mass change } (\Delta m) = (-1/2)(f_o^{-2})(\Delta f)\ A\ (k\rho)^{1/2} \qquad (2)$$

Where, A is the area of the gold disk coated onto the quartz crystal, ρ is the density of the crystal, k is the shear modulus of the crystal, Δf is the measured frequency change and f_o is the oscillation frequency of the crystal. A frequency change of 1 Hz is equivalent to a 1.4 ng change in mass [49–51]. From this value, the mass change during the deposition of $RuO_x\cdot nH_2O/IrCl_6^{2-}$ film, only Pt film and hybrid-II film on the gold electrodes for the first 6 cycles has been calculated as 0.49, 3.15 and 3.36 μg respectively. For all the three films, the increase in the voltammetric peak current and the frequency decrease (or mass increase) are found to be consistent with the growth of the films on the gold electrodes. Similarly, the change between consecutive scans $\Delta f_n - \Delta f_{n-1}$, clearly reveals that Δf changed at a constant rate during consecutive scans. These above EQCM results reveal that, the amount of deposition of $RuO_x\cdot nH_2O/IrCl_6^{2-}$ is enhanced in the presence of Pt.

3.3. Surface Morphological Characterization and EDX Analysis of $RuO_x \cdot nH_2O$, $RuO_x \cdot nH_2O/IrCl_6^{2-}$, and Hybrid-II Films

The microstructures of $RuO_x \cdot nH_2O$, $RuO_x \cdot nH_2O/IrCl_6^{2-}$ and hybrid-II films on indium tin oxide (ITO) have been characterized using SEM and AFM as shown in Figure 2. All the three films were prepared on ITOs at similar conditions as that of GC. The SEM and AFM studies of $RuO_x \cdot nH_2O$ (Fig. 2A and D) shows that electrosynthesized film has a structure with an average size of grains in the radii 1 μm. Similarly, in Figure 2B and E the $RuO_x \cdot nH_2O/IrCl_6^{2-}$ has smooth crystal shape structures as reported in the previous literature [52] however, it has non-uniform film. Figure 2C and F indicates that the spherical shapes of the Pt micro particles dispersed uniformly along with the $RuO_x \cdot nH_2O/IrCl_6^{2-}$ film, which shows the obvious formation of hybrid-II film. The average sizes of Pt grains are in the radii of 500 to 700 nm. From the AFM figures, the thickness of the $RuO_x \cdot nH_2O$, $RuO_x \cdot nH_2O/IrCl_6^{2-}$ and hybrid-II films have been found to be 55, 270 and 110 nm respectively. The cause of higher thickness of the $RuO_x \cdot nH_2O/IrCl_6^{2-}$ film is due to nonuniform deposition of $IrCl_6^{2-}$ when comparing in the hybrid-II film, which is consistent with EDX quantitative results given in Figure 2A, B and C insets. Where, in the Figure 2B inset, the EDX beam is focused on the bulky structure of $IrCl_6^{2-}$ (higher wt% of Ir and Cl). These SEM, AFM and EDX results along with EQCM results reveals that there is a uniform, smaller in size but more deposition of $RuO_x \cdot nH_2O$ and $IrCl_6^{2-}$ taken place in the presence of Pt. Similarly, the EDX results of hybrid-I film (not shown) reveals that there is less deposition of $RuO_x \cdot nH_2O$ and $IrCl_6^{2-}$ in hybrid-I film when comparing hybrid-II film. These results are consistent with the results obtained in CV characterization and the Γ values in Table. 1.

3.4. Electrocatalytic Oxidation Studies of Arsenic Oxide at $RuO_x \cdot nH_2O$, $RuO_x \cdot nH_2O/IrCl_6^{2-}$, and Hybrid-II Films

The electrocatalytic oxidation of arsenic oxide has been studied using $RuO_x \cdot nH_2O$, $RuO_x \cdot nH_2O/IrCl_6^{2-}$ and hybrid-II film modified GC electrodes. The As(III) oxidation

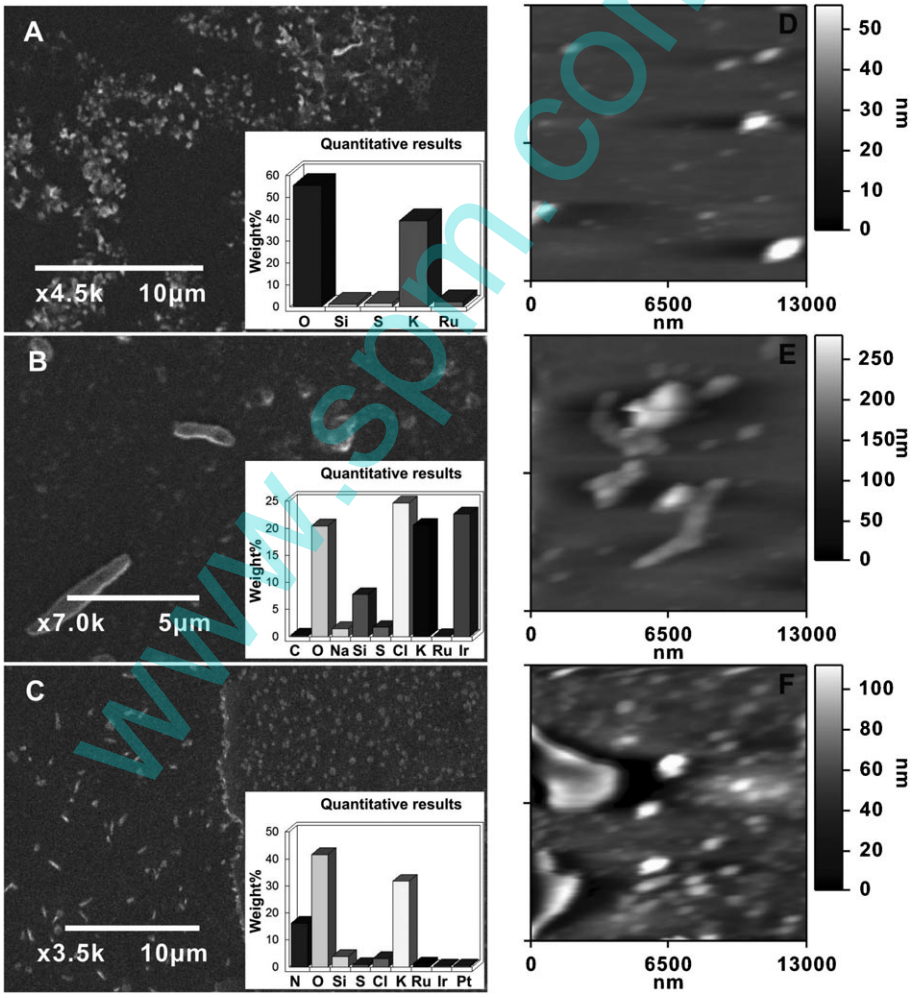

Fig. 2. SEM micrographs of ITO electrode surface modified with various films: A) $RuO_x \cdot nH_2O$, B) $RuO_x \cdot nH_2O/IrCl_6^{2-}$, and C) hybrid-II. Similarly D), E), and F) represent the AFM topographic images of $RuO_x \cdot nH_2O$, $RuO_x \cdot nH_2O/IrCl_6^{2-}$, and hybrid-II films respectively. The inset graphs in A, B, and C are the quantitative results obtained from the EDX spectrum of respective films.

was carried out in pH 2.0 buffer solution containing $NaAsO_2$. Figure 3A shows the CVs of hybrid-II film in the presence and absence of AsO_2^-. In the absence of AsO_2^- Figure 3Aa, the hybrid-II film exhibit only the redox couples $E^{\circ\prime} = -0.08$ and -0.18 V. Upon the addition of $NaAsO_2$ two new anodic peaks of AsO_2^- at $E_{pc} = 0.1$ and 0.8 V has been obtained. The increasing concentration of $NaAsO_2$ (20 to 130 μM) increases both anodic peak currents, while the cathodic peak currents decrease. When comparing this above result with the bare GC (a'), no voltammetric signal has been observed for bare GC within the potential range of AsO_2^- oxidation (at 130 μM). The inset in Figure 3A represents the AsO_2^- oxidation peak current at $E_{pc} = 0.8$ V, where a, b, and c represents hybrid-II, $RuO_x \cdot nH_2O/IrCl_6^{2-}$ and $RuO_x \cdot nH_2O$ films respectively. This inset reveals that hybrid-II film modified electrode possess high electrocatalytic oxidation current for AsO_2^- than the $RuO_x \cdot nH_2O$, $RuO_x \cdot nH_2O/IrCl_6^{2-}$ modified GC electrodes. Martel et. al., reported that the presence of Pt particles increased the oxidation current of As(III) at $P_2Mo_{18}O_{62}^{6-}$ hybrid film and protonated 1,12-diamino-dodecane $(NH_2\text{-}(CH_2)_{12}\text{-}NH_2)$/Pt modified electrode [53]. Hence, this phenomenon could be due to the increase of active sites in the presence of Pt.

3.5. RDE and $i-t$ Curve Studies of Arsenic Oxide at Hybrid-II Film

A detailed study of arsenic oxide oxidation has been carried out using rotating disk electrode (RDE) technique. Figure 3B shows the electrocatalytic oxidation of arsenic oxide at different rotation speeds (200 to 2500 rpm) at the hybrid-II film in 0.1 M KNO_3 solution (pH 2.0). The inset shows the Levich plot obtained for the above mentioned voltammograms, which is found to be linear. If the electron transfer process of the hybrid-II film is assumed to be fast, in tune with the experimental conditions, then the rate determining step must have been one of following, i) mass transfer process of arsenic oxide in the solution, ii) catalytic process at the film/solution interface or iii) Electron diffusion problem within the film. In case, the oxidation of arsenic oxide at hybrid-II film controlled solely by the mass transfer process in the solution, then the relationship between the limiting current and rotating speed should obey the following Levich equation

$$I_L = 0.62nFAD^{2/3}\omega^{-1/2}v^{-1/6}c_0 \quad (3)$$

Where, n number of electrons (assumed as 2), F faraday constant, A area of disk electrode (0.16 cm^2), D diffusion coefficient, ω angular velocity of the electrode, v kinematic viscosity, c_0 bulk concentration of arsenic oxide (0.4 mM). Similarly, the following equation [54] can be used to calculate the rate constant

$$I_k = nFAk\Gamma c_0 \quad (4)$$

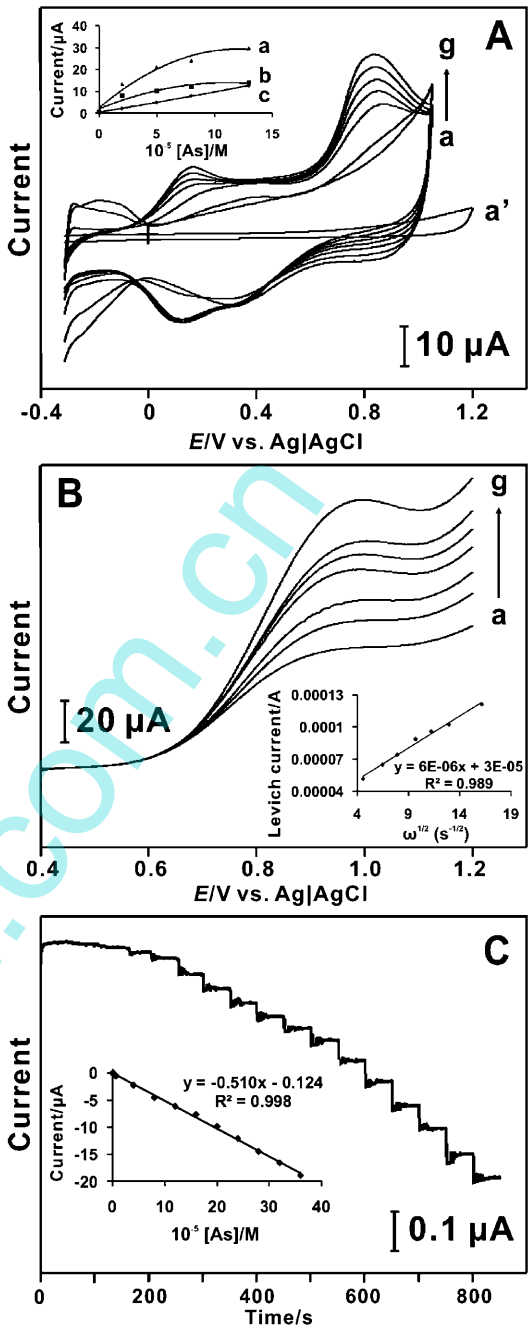

Fig. 3. A) CVs of hybrid-II film on GC in 0.1 M KNO_3 at pH 2.0 with various concentrations of $[NaAsO_2]$ = a) 0.0, b) 0.2, c) 0.5, d) 0.8, e) 1.1, f) 1.4, and g) 1.7 mM. a') bare GC and $[NaAsO_2]$ = 1.7 mM. Scan rate = 100 mV s^{-1}. Inset in A) shows the plot of current vs. different concentrations of $NaAsO_2$ at a) hybrid-II, b) $RuO_x \cdot nH_2O/IrCl_6^{2-}$, and c) $RuO_x \cdot nH_2O$ films. B) RDE voltammogram of a hybrid-II GC disk electrode for 0.4 mM $[NaAsO_2]$ in 0.1 M KNO_3 pH 2.0 solution. Rotation rate = a) 200, b) 400, c) 600, d) 900, e) 1200, f) 1600, and g) 2500 rpm. Scan rate = 10 mV s^{-1}. Inset in (B) shows a plot of Levich current vs. rotation rate. C) Amperometric responses of 16 sequential additions of $NaAsO_2$ (20 nM to 6.8 μM) at hybrid-II film modified GC in 0.1 M KNO_3 at pH 2.0 (0.85 V). Rotating rate: 600 rpm. Inset: Relationship between oxidation current vs. $[NaAsO_2]$ obtained from 25 additions in the concentration range of 20 nM to 0.36 mM.

Where, k is the rate constant and Γ is the surface coverage concentration of the catalyst in hybrid-II film (from Table 1). From these above values and equations, the diffusion coefficient and the rate constant values of arsenic oxide at different films has been calculated and given in Table 2. These obtained values are lower than the previously reported values [55, 56]. However, there is a lower in over potential of the arsenic oxide at hybrid-II film (in CV) when comparing with the previously reported values.

Steady state current response for the oxidation of AsO_2^- at the hybrid-II film modified electrode was carried out and the results are presented in Figure 3C. The concentration of AsO_2^- was increased by successive injection of $NaAsO_2$ (60 nM to 6.8 μM) into 0.1 M KNO_3 at pH 2.0 aqueous. The oxidation of AsO_2^- was examined by holding the modified electrode potential at 0.85 V. The amperometric response was reached in about 5 s upon the addition of $NaAsO_2$, also the response was proportional to the $NaAsO_2$ concentration. Whereas, there is no response for the $NaAsO_2$ at bare GC (figure not shown). The slope in the inset of Figure 3C is 51 μA mM^{-1} with a correlation coefficient of 0.998, where $n = 25$. From the slope value, the sensitivity of the hybrid-II film for AsO_2^- oxidation has been calculated as 0.7 mA $mM^{-1}cm^{-2}$, which is efficient than the recently reported values at cobalt oxide nanoparticles modified electrodes (111.3 nA μM^{-1}) [57] and iodide film modified electrodes (0.43 μA μM^{-1}) [58]. Similarly, the detection limit using i-t curve is found to be 60 nM of $NaAsO_2$ at a signal to noise ratio of 3. From all these above results, it is obvious that AsO_2^- has been oxidized by hybrid-II film through mediated action of three components Pt, $RuO_x \cdot nH_2O$, and $IrCl_6^{2-}$.

3.6. Electrocatalytic Oxidation Studies of Methanol at $RuO_x \cdot nH_2O$, $RuO_x \cdot nH_2O/IrCl_6^{2-}$, and Hybrid-II Films

The oxidation of different concentrations of methanol at $RuO_x \cdot nH_2O$, $RuO_x \cdot nH_2O/IrCl_6^{2-}$ and hybrid-II films in aqueous solution (pH 2.0) has been studied. In the absence of methanol all the three films shows their respective redox couples as discussed in the electrochemical characterization section. Upon the addition of methanol, the oxidation peak appeared at 0.5 V. As the concentration of methanol increased (0.1 to 0.3 M), the anodic peak current of hybrid-II film (Fig. 4A) at 0.5 V increased noticeably. But the increase of peak current (same potential) of methanol at $RuO_x \cdot nH_2O$ and $RuO_x \cdot nH_2O/IrCl_6^{2-}$ is not higher than the hybrid-II film (figures not shown). Similarly, the bare GC (a') has no voltammetric signal within the potential range of methanol oxidation (at 0.3 M). The mechanism involved in the methanol oxidation at hybrid-II film could be given by

$$CH_3OH \rightarrow CO_{ads} + 4H^+ + e^- \quad (5)$$

$$CO_{ads} + H_2O \rightarrow CO_2 + 2H^+ + 2\ e^- \quad (6)$$

From these results, it is clear that the oxidation of methanol by hybrid-II film is obvious than that of $RuO_x \cdot nH_2O$ and $RuO_x \cdot nH_2O/IrCl_6^{2-}$ films. For hybrid-II film, the slope from the Tafel plot (not shown in figure) has the ca. value of 120 mV dec^{-1}. In the recent investigation under similar experimental conditions but using a commercial Pt-Ru/C powder, a value of 124 mV dec^{-1} was observed for $RuO_x \cdot nH_2O/IrCl_6^{2-}$ film modified electrode [59, 60].

3.7. Electrocatalytic Reduction Studies of Oxygen at $RuO_x \cdot nH_2O$, $RuO_x \cdot nH_2O/IrCl_6^{2-}$, and Hybrid-II Films

The electrocatalytic reduction of oxygen has been studied using $RuO_x \cdot nH_2O$, $RuO_x \cdot nH_2O/IrCl_6^{2-}$ and hybrid-II film modified GC electrodes. The CVs have been carried using aqueous buffer solution of pH 2.0. The reduction reaction of O_2 (240 μM) is absent at both $RuO_x \cdot nH_2O$ and $RuO_x \cdot nH_2O/IrCl_6^{2-}$ films (figures not shown). Figure 4B shows the CVs of hybrid-II film in the presence and absence of oxygen. The absence of O_2 in Figure 4Ba, the hybrid-II film exhibits two redox couples ($E^{\circ\prime} = -0.08$ and -0.18 V) and two cathodic peak currents $E_{pc} = 0.35$ and 0.8 V. Upon the addition of O_2, two new oxidation peaks of O_2 at $E_{pc} = 0.3$ and 0.85 V has been obtained. The increasing concentration of O_2 (40 to 240 μM) increases both cathodic peak currents. The slope in the inset of Figure 4B is 137 μA mM^{-1} with a correlation coefficient of 1.0, where $n = 6$. From the slope value, the sensitivity of hybrid-II film for O_2 reduction has been calculated as 1.8 mA $mM^{-1}cm^{-2}$. This catalytic phenomenon of the hybrid-II films towards O_2 is because of the presence of Pt. In hybrid-II film, the oxide layer formation on the metal surface could be explained as H_2O oxidation. Based on this argument, the electrochemical reduction from O_2 to H_2O by Pt and Pt oxide layer could be given by

$$PtO + 2H^+ + 2e^- \rightarrow Pt + H_2O \quad (7)$$

Table 2. Diffusion coefficient and rate constant values of different analytes at different film modified electrodes in 0.1 M KNO_3 at pH 2.0.

Analyte type	Film type	Diffusion coefficient ($cm^2\ s^{-1}$)	Rate constant ($M^{-1}\ s^{-1}$)
$NaAsO_2$	$RuO_x \cdot nH_2O$	3.78×10^{-12}	8.83×10^3
	$RuO_x \cdot nH_2O/IrCl_6^{2-}$	1.67×10^{-10}	2.25×10^4
	Hybrid-II	1.93×10^{-10}	1.26×10^4
O_2	Hybrid-II	1.02×10^{-9}	1.53×10^2

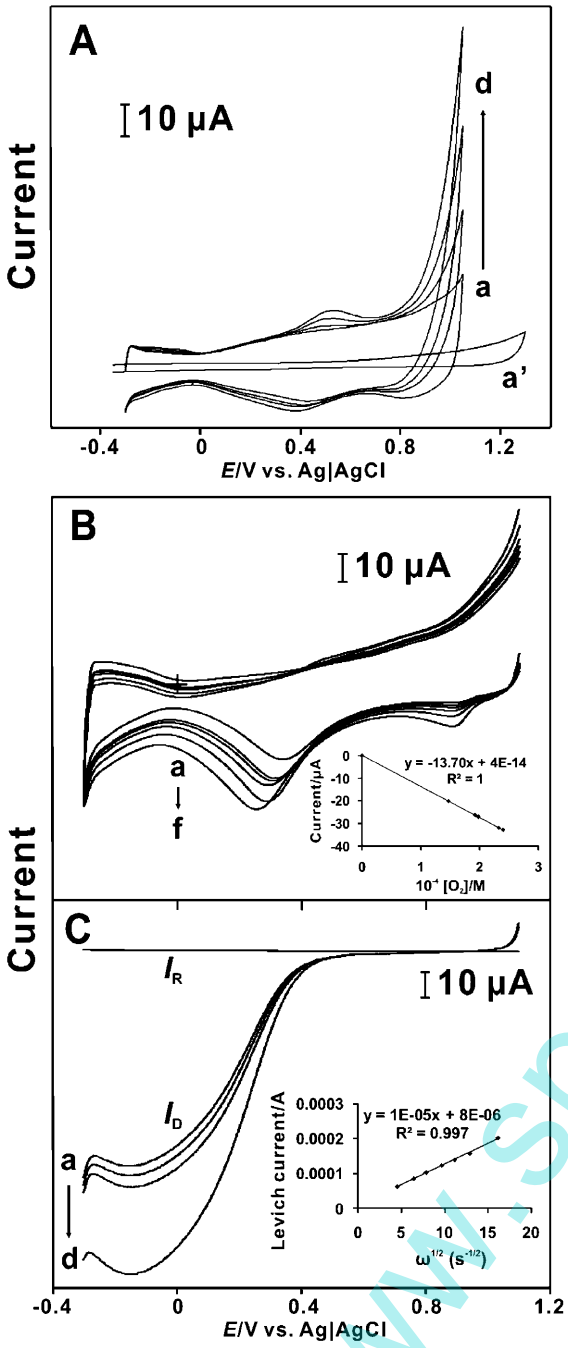

Fig. 4. CVs of A) hybrid-II film modified GC electrodes in 0.1 M KNO_3 at pH 2.0 with various concentrations of $[CH_3OH]$ = a) 0.0, b) 0.1, c) 0.2, and d) 0.3 M. a') represents bare glassy electrode and $[CH_3OH] = 0.3$ M. Scan rate = 100 mV s^{-1}. B) Hybrid-II film modified GC at similar conditions with various concentrations of $[O_2]$ = a) 0.0, b) 40, c) 80, d) 120, e) 160, and f) 240 μM. Scan rate = 100 mV s^{-1}. Inset in (B) shows the plot of current vs. different concentrations of O_2 at hybrid-II film. C) RRDE voltammogram of hybrid-II modified GC disk electrode in 0.1 M KNO_3 at pH 2.0 with different concentrations of $[O_2]$ = a) 0, b) 120, c) 160, and d) 240 μM. Scan rate = 10 mV s^{-1}. I_R and I_D represent the ring current and disk current respectively, where $E_R = 0.7$ V. Inset in (C) shows a plot of Levich current vs. rotation rate for hybrid-II GC disk electrode for 240 μM $[O_2]$; Rotation rate = a) 200, b) 400, c) 600, d) 900, e) 1200, f) 1600, and g) 2500 rpm. Scan rate = 10 mV s^{-1}.

$$Pt + 2H^+ + O_2 \rightarrow PtO + H_2O \quad (8)$$

Figure 4C shows the electrochemical reduction of O_2 by hybrid-II film modified GC disk electrode (at 0.25 V) and electrochemical oxidation of H_2O_2 by bare platinum ring electrode (at 0.7 V) in an aqueous buffer solution at pH 2.0. The increase in concentration of O_2 increases the disk current (I_D). However, the platinum ring current (I_R), does not show obvious increase during the increase of O_2 concentration. This result shows that H_2O_2 is not formed during the reduction of O_2. From this argument, the reduction mechanism of O_2 on the hybrid-II could be proposed by the following equation

$$O_2 + 4e^- + 4H^+ \rightarrow 2H_2O \quad (9)$$

The RDE studies for the O_2 reduction reactions have been carried out at different rotation speeds (200 to 2500 rpm) at the hybrid-II film in 0.1 M KNO_3 solution (pH 2.0). The inset in Figure 4C shows the Levich plot obtained for the above mentioned voltammograms is found to be linear. As we discussed in the RDE studies for arsenic oxide, the O_2 is also considered as controlled by the mass transfer process in the solution. From the Equations 3 and 4, the diffusion coefficient and rate constant (where, Γ is taken from Table 1) has been calculated for the O_2 reduction at hybrid-II film and given in Table 2; where the bulk concentration of the analyte is 240 μM. These obtained values are lower than the previously reported values [61, 62].

4. Conclusions

$RuO_x \cdot nH_2O/IrCl_6^{2-}$/Pt hybrid film (hybrid-II) containing enhanced electrocatalytic property has been prepared by CV technique on GC, gold and ITO electrodes. The prepared film shows excellent electrochemical properties in pH 2.0 aqueous solution. The EQCM results show that the amount of $RuO_x \cdot nH_2O/IrCl_6^{2-}$ has been enhanced in the presence of Pt. The SEM, AFM and EDX studies show the presence of dispersed Pt particles along with the uniform $RuO_x \cdot nH_2O/IrCl_6^{2-}$ film. In the hybrid-II modified electrode, $RuO_x \cdot nH_2O/IrCl_6^{2-}$ plays an important role in the mediated oxidation of arsenic oxide. The presence of Pt particles increased the active sites for electrochemical oxidation of arsenic oxide and thereby increased the electrocatalytic oxidation current. The hybrid-II films have also shown enhanced catalytic activity towards methanol oxidation and oxygen reduction reactions. The enhancement of these catalytic reactions is due to the presence of Pt particles in the hybrid film.

5. Acknowledgements

This work was supported by the National Science Council and the Ministry of Education of Taiwan (Republic of China).

6. References

[1] Z. Jusys, R. J. Behm, *Electrochim. Acta* **2004**, *49*, 3891.
[2] L. Xiong, A. Manthiram, *Electrochim. Acta* **2004**, *49*, 4163.
[3] E. V. Spinac'e, A. O. Neto, M. Linardi, *J. Power Sources* **2004**, *129*, 121.
[4] Y. Takasu, T. Kawaguchi, W. Sugimoto, Y. Murakami, *Electrochim. Acta* **2003**, *48*, 3861.
[5] K. W. Park, B. K. Kwon, J. H. Choi, I. S. Park, Y. M. Kim, Y. E. Sung, *J. Power Sources* **2002**, *109*, 439.
[6] K. Shukla, R. K. Raman, N. A. Choudhury, K. R. Priolkar, P. R. Sarode, S. Emura, R. Kumashiro, *J. Electroanal. Chem.* **2004**, *563*, 181.
[7] E. V. Spinac'e, A. O. Neto, T. R. R. Vasconcelos, M. Linardi, *J. Power Sources* **2004**, *137*, 17.
[8] W. Zhou, Z. Zhou, S. Song, W. Li, G. Sun, P. Tsiakaras and Q. Xin, *Appl. Catal. B: Environ.* **2003**, *46*, 273.
[9] L. Gao, H. Huang, C. Korzeniewski, *Electrochim. Acta* **2004**, *49*, 1281.
[10] S. L. Gojkovic, T. R. Vidakovic, D. R. Durovic, *Electrochim. Acta* **2003**, *48*, 3607.
[11] A. Yu, Z. Liang, J. Cho, F. Caruso, *Nano Lett.* **2003**, *3*, 1203.
[12] Y. Xiao, H. X. Ju, H. Y. Chen, *Anal. Chim. Acta* **1999**, *391*, 73.
[13] L. R. Hilliard, X. Zhao, W. Tan, *Anal. Chim. Acta* **2002**, *470*, 51.
[14] M. Qhobosheane, S. Santra, P. Zhang, W. Tan, *Analyst* **2001**, *126*, 1274.
[15] S. Dong, *Chemically Modified Electrodes*, Science Publishers, Beijing **1993**, pp. 260.
[16] R. Garjonyte, A. Malinauskas, *Sens. Actuators B* **1998**, *46*, 236.
[17] S. M. Chen, C. M. Chan, *J. Electroanal. Chem.* **2003**, *543*, 161.
[18] S. M. Chen, M. F. Lu, K. C. Lin, *J. Electroanal. Chem.* **2005**, *579*, 163.
[19] N. R. de Tacconi, K. Rajeshwar, R. O. Lezna, *Electrochim. Acta* **2000**, *45*, 3403.
[20] K. M. Jeerage, W. A. Steen, D. T. Schwartz, *Chem. Mater.* **2002**, *14*, 530.
[21] M. Jeyalakshmi, F. Scholz, *J. Power Sources* **2000**, *91*, 217.
[22] H. B. Suffredini, V. Tricoli, L. A. Avaca, N. Vatistas, *Electrochem. Commun.* **2004**, *6*, 1025.
[23] H. B. Suffredini, J. L. Cerne, F. Crnkovic, S. A. S. Machado, L. A. Avaca, *J. Hydrogen Energy* **2000**, *25*, 415.
[24] M. Fallet, H. Mahdjoub, B. Gautier, J. P. Bauer, *J. Non-Crystalline Sol.* **2001**, *293*, 527.
[25] F. L. Perdomo, P. de Lima-Neto, M. A. Aegerter, L. A. Avaca, *J. Sol-Gel Sci. Tech.* **1999**, *15*, 87.
[26] M. Atik, P. de Lima-Neto, L. A. Avaca, M. A. Aegerter, *J. Appl. Electrochem.* **1995**, *25*, 142.
[27] K. Kameyama, S. Shohji, S. Onoue, K. Nishimura, K. Yahikozawa, Y. Takasu, *J. Electrochem. Soc.* **1993**, *140*, 1034.
[28] Y. Murakami, H. Ohkawauchi, M. Ito, K. Yahikozawa, Y. Takasu, *Electrochim. Acta* **1994**, *39*, 2551.
[29] Y. Takasu, S. Onoue, K. Kameyama, Y. Murakami, K. Yahikozawa, *Electrochim. Acta* **1994**, *39*, 1993.
[30] M. Guglielmi, P. Colombo, V. Rigato, G. Battaglin, A. Boscolo-Boscoletto, A. DeBattisti, *J. Electrochem. Soc.* **1992**, *139*, 165.
[31] K. Kameyama, K. Tsukada, K. Yahikozawa and Y. Takasu, *J. Electrochem. Soc.* **1994**, *141*, 643.
[32] R. KoÈ tz, S. Stucki, *Electrochim. Acta* **1986**, *31*, 1311.
[33] C. Angelinetta, M. Falciola, S. Trasatti, *J. Electroanal. Chem.* **1986**, *205*, 347.
[34] T. C. Wen, C. C. Hu, *J. Electrochem. Soc.* **1992**, *139*, 2158.
[35] K. Mandal, K. T. Suzuki, *Talanta* **2002**, *58*, 201.
[36] A. Davis, D. Sherwin, R. Ditmars, K. A. Hoenke, *Environ. Sci. Technol.* **2001**, *35*, 2401.
[37] T. Yoshida, H. Yamaguchi, G. F. Sunc, *Toxicol. Appl. Pharmacol.* **2004**, *198*, 243.
[38] A. Basu, J. Mahata, S. Gupta, A. K. Giri, *Mutat. Res.* **2001**, *488*, 171.
[39] K. Mandal, Y. Ogra, K. Anzai, K. T. Suzuki, *Toxicol. Appl. Pharmacol.* **2004**, *198*, 307.
[40] A. Salimi, H. Mamkhezri, R. Hallaj, S. Soltanian, *Sens. Actuatots B* **2008**, *129*, 246.
[41] T. A. Ivandini, R. Sato, Y. Makide, A. Fujishima, Y. Einaga, *Anal. Chem.* **2006**, *78*, 6291.
[42] J. -M. Zen, P. -Y. Chen, A. S. Kumar, *Anal. Chem.* **2003**, *75*, 6017.
[43] D. Zhang, D. Chi, T. Okajima, T. Ohsaka, *Electrochim. Acta* **2007**, *52*, 5400.
[44] J. Collman, L. Fu, P. Herrmann, X. Zhang, *Science* **1997**, *275*, 949.
[45] J. Zagal, M. P'aez, *J. Electroanal. Chem.* **1992**, *339*, 13.
[46] A. Bauer, E. L. Gyenge, C. W. Oloman, *J. Power Sources* **2007**, *167*, 281.
[47] L.-M. Huang, T. -C. Wen, *J. Power Sources* **2008**, *182*, 32.
[48] P. Shakkthivel, S. M. Chen, *Biosens. Bioelectron.* **2007**, *22*, 1680.
[49] U. Yogeswaran, S. M. Chen, *J. Electrochem. Soc.* **2007**, *154*, E178.
[50] S. M. Chen, M. I. Liu, *Electrochim. Acta* **2006**, *51*, 4744.
[51] S. M. Chen, C. J. Liao, V. S. Vasantha, *J. Electroanal. Chem.* **2006**, *589*, 15.
[52] C. Hu, Y. H. Huang, *J. Electrochem. Soc.* **1999**, *146*, 2465.
[53] D. Martel, A. Kuhn, P. J. Kulesza, M. T. Galkowski, M. A. Malik, *Electrochim. Acta* **2001**, *46*, 4197.
[54] H. W. Chu, R. Thangamuthu, S. M. Chen, *Electrochim. Acta* **2008**, *53*, 2862.
[55] F. Brusciotti, P. Duby, *Electrochim. Acta* **2007**, *52*, 6644.
[56] G. Hignett, J. D. Wadhawan, N. S. Lawrence, D. Q. Hung, C. Prado, F. Marken, R. G. Compton, *Electroanalysis* **2004**, *16*, 897.
[57] A. Salimi, H. Mamkhezri, R. Hallaj, S. Soltanian, *Sens. Actuators B* **2008**, *129*, 246.
[58] B. W. Su, S. Thiagarajan, S. M. Chen, *J. Electrochem. Soc.* **2008**, *155*, F157.
[59] G. Wu, L. Li, B. Q. Xu, *Electrochim. Acta* **2004**, *50*, 1.
[60] W. Sugimoto, T. Saida, Y. Takasu, *Electrochem. Commun.* **2006**, *8*, 411.
[61] A. Sarapuua, A. Kasikovb, T. Laaksonenc, K. Kontturic, K. Tammeveski, *Electrochim. Acta* **2008**, *53*, 5873.
[62] S. Tsujimura, Y. Miura, K. Kano, *Electrochim. Acta* **2008**, *53*, 5716.

